Remote Sensing of Environment 140 (2014) 625–638

Contents lists available at ScienceDirect

Remote Sensing of Environment

journal homepage: www.elsevier.com/locate/rse

MODIS time-series-derived indicators for the beginning of the growing season in boreal coniferous forest — A comparison with CO_2 flux measurements and phenological observations in Finland

Kristin Böttcher [a,*], Mika Aurela [b], Mikko Kervinen [a], Tiina Markkanen [b], Olli-Pekka Mattila [a], Pasi Kolari [c], Sari Metsämäki [a], Tuula Aalto [b], Ali Nadir Arslan [b], Jouni Pulliainen [b]

[a] Finnish Environment Institute, Geoinformatics Division, FI-00251 Helsinki, Finland
[b] Finnish Meteorological Institute, FI-00560 Helsinki, Finland
[c] University of Helsinki, Forest Sciences, FI-00014 University of Helsinki, Finland

ARTICLE INFO

Article history:
Received 14 June 2012
Received in revised form 25 September 2013
Accepted 26 September 2013
Available online 25 October 2013

Keywords:
Boreal forest
Vegetation phenology
Growing season onset
Fractional snow cover

ABSTRACT

Spring phenological events are important for the assessment of the carbon budget in forest ecosystems. In large parts of the boreal zone the evergreen conifers are dominant, but most available satellite-based methods for the detection of the start of the growing season have focussed on the greening-up of deciduous species. We investigated the possibility of determining spring phenological events of boreal evergreen coniferous forest from Moderate Resolution Imaging Spectroradiometer (MODIS) time-series based on test sites in Finland. The beginning of the photosynthetically active period, determined from the CO_2 fluxes measured with the eddy covariance (EC) method, was used as a primary reference for the onset of the growing season (growing season start date, GSSD). Furthermore, phenological observations of pine trees, such as the beginning of shoot elongation (growth of pine start date, GPSD) were included in the comparison. The corresponding indicators were derived from MODIS data and compared with *in situ* phenological observations. This was carried out using cloud-filtered daily MODIS time-series of Normalized Difference Vegetation Index (NDVI), Normalized Difference Water Index (NDWI) and Fractional Snow Cover (FSC) from homogenous areas around *in situ* sites (3 EC sites and 4 phenological sites in Finland). GSSD in coniferous forest showed correspondence with the time during snowmelt when the ground starts to be exposed, which was indicated by a decrease in FSC and the spring-rise in NDVI time-series. GPSD occurred in general after complete snow melt. Satellite-derived GSSD from NDVI ($GSSD_{NDVI}$) and FSC ($GSSD_{FSC}$) showed good correspondence with *in situ* observations for both NDVI and FSC ($R^2 > 0.8$, RMSE < 7 days) including observations from two CO_2 flux measurement sites in Northern Finland and one in Southern Finland. The highest site-wise correlations were obtained for the satellite indicator $GSSD_{FSC}$. Finally, the national-scale mapping of GSSD was demonstrated based on the satellite-derived indicator $GSSD_{FSC}$.

1. Introduction

Spring phenology is one important factor influencing the carbon balance of boreal forest ecosystems (Richardson et al., 2009, 2010) and therefore accurate information related to spring phenology is needed for studies of the carbon budget of this region. The recovery of photosynthetic activity (referred here as growing season start date, GSSD) in an ecosystem can be determined from *in situ* eddy covariance (EC) measurements of the CO_2 fluxes at local sites (e.g. Suni et al., 2003). These point-wise measurements need to be generalised to larger areas and satellite observations could be one possibility to achieve that.

Time-series of vegetation indices, such as the Normalized Difference Vegetation Index (NDVI), are widely used for monitoring of vegetation phenology (Badeck et al., 2004; Reed et al., 1994; White, Thornton, & Running, 1997). The NDVI eliminates dependence on sun–target–sensor geometry to a certain extent, but due to differences in the anisotropic behaviour of canopies in red and near-infrared reflectance, NDVI is slightly geometry-dependent (Gutman, 1991). The sensitivity of NDVI to sun zenith angle (SZA) is low (Huemmrich, Black, Jarvis, McCaughey, & Hall, 1999) and depends on the leaf area of the canopy and reflectivity of the ground. The influence of SZA decreases with increasing canopy leaf area and darker ground (Kaufmann et al., 2000). The contrast between red and near-infrared reflectance is reduced by atmospheric effects, which usually lead to lower NDVI (Gutman, 1991). According to theoretical analysis by Sellers (1985), NDVI can be directly related to photosynthesis in non-water-limited environments; correlations between NDVI and gross primary production (GPP) (Wang et al., 2004) and modelled photosynthetic capacity in boreal forests (Gea-Izquierdo et al., 2010) were reported. For the extraction of phenological key-stages of vegetation from NDVI time-series, such as

* Corresponding author. Tel.: +358 401 876447; fax: +358 9 40300690.
E-mail address: kristin.bottcher@environment.fi (K. Böttcher).

0034-4257/$ – see front matter © 2013 Elsevier Inc. All rights reserved.
http://dx.doi.org/10.1016/j.rse.2013.09.022

onset of greenness, good correspondence has been obtained between satellite-derived budburst day and field observations for deciduous trees in the temperate region (Badeck et al., 2004; Duchemin, Goubier, & Courrier, 1999; Maignan, Bréon, Bacour, Demarty, & Poirson, 2008; Soudani et al., 2008).

However, in the boreal region greening-up and snow melt cannot be well distinguished in NDVI time-series (Delbart, Kergoat, Le Toan, L'Hermitte, & Picard, 2005; Jönsson, Eklundh, Hellström, Bärring, & Jönsson, 2010; Moulin, Kergoat, Viovy, & Dedieu, 1997; White et al., 2009), because the NDVI already shows a steep increase when snow melts, due to a strong decrease in reflectance. Therefore adapted methods were developed to determine the greening-up in this region (Beck, Atzberger, Høgda, Johansen, & Skidmore, 2006; Delbart et al., 2005; Karlsen et al., 2008). In order to avoid the influence of snow cover on the retrieval of the greening-up, Delbart et al. (2005) developed a method based on the Normalized Difference Vegetation Index (NDWI). NDWI was initially applied for the monitoring of vegetation liquid water content from space using radiances at wavelengths 860 nm and 1240 nm (Gao, 1996). Both wavelengths are located in the reflectance plateau of vegetation canopies and therefore sense similar depth through vegetation canopies, in contrast to NDVI for which the red channel is located in the strong chlorophyll absorption region. NDWI is less sensitive to atmospheric scattering than NDVI (Gao, 1996). It decreases during snowmelt and increases when vegetation is greening up, thus allowing a free-of snow effect determination of greening-up in the boreal region (Delbart et al., 2005).

In contrast to deciduous trees, seasonal changes in evergreen conifers are not easily observed. Photosynthesis is inhibited during winter, but close-to-full photosynthetic capacity can be reached only after a few days with optimal environmental conditions (Sevanto et al., 2006). Photosynthetic recovery is mainly driven by air temperature (Suni et al., 2003), independent from changes in canopy structure (Richardson et al., 2009), includes multiple steps and is reversible (Monson et al., 2005). While air temperature was found to be the main factor for the onset of photosynthesis, soil temperature is an important limiting factor for full photosynthetic recovery in late spring after the end of the snow melt (Bergh & Linder, 1999; Wu, Jansson, & Kolari, 2012).

Differences in the beginning of the growing season between evergreen coniferous forests and other vegetation species, such as deciduous broadleaved forest, were mostly overlooked in mapping of this event from satellite-derived time-series, and the same methodology (using in general bud burst observation of deciduous trees as reference) was applied for different land cover classes and regions, for example in the MODIS phenology product (Ganguly, Friedl, Tan, Zhang, & Verma, 2010). Comparisons between springtime source-sink transition indicators derived from CO_2 flux measurements and satellite-derived phenological indicators across deciduous broadleaved and evergreen coniferous forest sites showed correlations for both ecosystems, but the flux-derived date in evergreen coniferous forests preceded the satellite-derived indicator by several weeks (Melaas et al., 2013; Richardson et al., 2010).

The satellite-derived greening-up in evergreen coniferous forest may correspond to the start of needle growth (Beck et al., 2007), but satellite-retrievals were usually not verified with phenological observations of evergreen conifers (Gonsamo, Chen, Price, Kurz, & Wu, 2012). Only a few studies compared spring phenological events in evergreen coniferous forest with satellite-derived time series (Gonsamo et al., 2012; Jönsson et al., 2010; Thum et al., 2009). The timing of budburst of evergreen conifers in Swedish forest could not be derived with absolute nor relative threshold values of vegetation indices, due to the influence of snow cover and the small and slow changes of needle biomass (Jönsson et al., 2010). Thum et al. (2009) found that the beginning of snow melt, determined from Moderate Resolution Imaging Spectrometer (MODIS) surface albedo observations, appeared to be a good estimator for the beginning of the active period of coniferous forest as observed from EC measurements.

The aim of this work was therefore to evaluate the possibility to use satellite-derived proxy indicators for the determination of GSSD in evergreen coniferous forest in the boreal region. A special interest of this paper was to investigate the feasibility of using the Earth observation-based Fractional Snow Cover (FSC) product as indicator for GSSD. The applied FSC estimates are derived with the reflectance model-based snow monitoring method SCA*mod* (Metsämäki, Anttila, Huttunen, & Vepsäläinen, 2005) of the Finnish Environment Institute (SYKE), developed for boreal forest and the tundra belt. It has been shown to provide reliable estimates of the fractional snow cover for forested areas; validation against ground truth data from distributed snow surveys in Finland showed a root mean squared error (RMSE) of 0.11 FSC and higher retrieval accuracies for boreal forests than e.g. the MODIS fractional snow cover product by NASA/Goddard Space Flight Center (Hall & Riggs, 2007; Riggs, Hall, & Salomonson, 2006) were demonstrated (Metsämäki et al., 2012). Hence, MODIS-derived time-series of FSC, as well as commonly used vegetation indices such as NDVI and NDWI, were compared with *in situ* dates of GSSD from three EC sites in order to develop a method for the detection of GSSD from satellite-derived time-series. In order to allow comparisons with other studies

Table 1
Characteristics of *in situ* sites.

Site	Observation/ organisation	Geographic coordinates	Altitude above sea (m)	Forest type	Phytogeographical zone[1]	Mean annual air temperature (°C) and precipitation (mm)[2]	Observation period
Äkäslompolo	Phenology/METLA	67° 35′ N 24° 12′ E	340	Scots pine	Northern boreal	−1.4[a] 484	2001–2006
Hyytiälä	CO_2 flux/ University of Helsinki	61° 51′ N 24° 17′ E	170	Scots pine/ Norway spruce	Southern boreal	3.5[b] 601	2001–2010
Kenttärova	CO_2 flux/FMI	67° 59′ N 24° 15′ E	347	Norway spruce	Northern boreal	−1.8[c] 501	2003–2010
Paljakka	Phenology/METLA	64° 40′ N 28° 03′ E	295	Scots pine	Middle boreal	1.7[d] 532	2001–2010
Parkano	Phenology/METLA	62° 01′ N 23° 03′ E	115	Scots pine	Southern boreal	2.7[e] 632	2001–2008, 2010
Saariselkä	Phenology/METLA	68° 24′ N 27° 23′ E	300	Scots pine	Northern boreal	−0.8[f] 435	2001–2006
Sodankylä	CO_2 flux/FMI	67° 21′ N 26° 38′ E	179	Scots pine	Northern boreal	−0.8 507	2001–2010

METLA, Finnish Forest Research Institute. FMI, Finnish Meteorological Institute.
[1] Definition of phytogeographical zones according to Ahti, Hämet-Ahti, and Jalas (1968).
[2] Long term records of air temperature and precipitation are for the period from 1971 to 2000 from stations: [a]Muonio Alamuonio, [b]Jämsä, [c]Kittilä Pulju, [d]Kajaani airport, [e]Ähtäri Myllymäki, [f]Inari/Ivalo airport (Drebs, Nordlund, Karlsson, Helminen, & Rissanen, 2002).

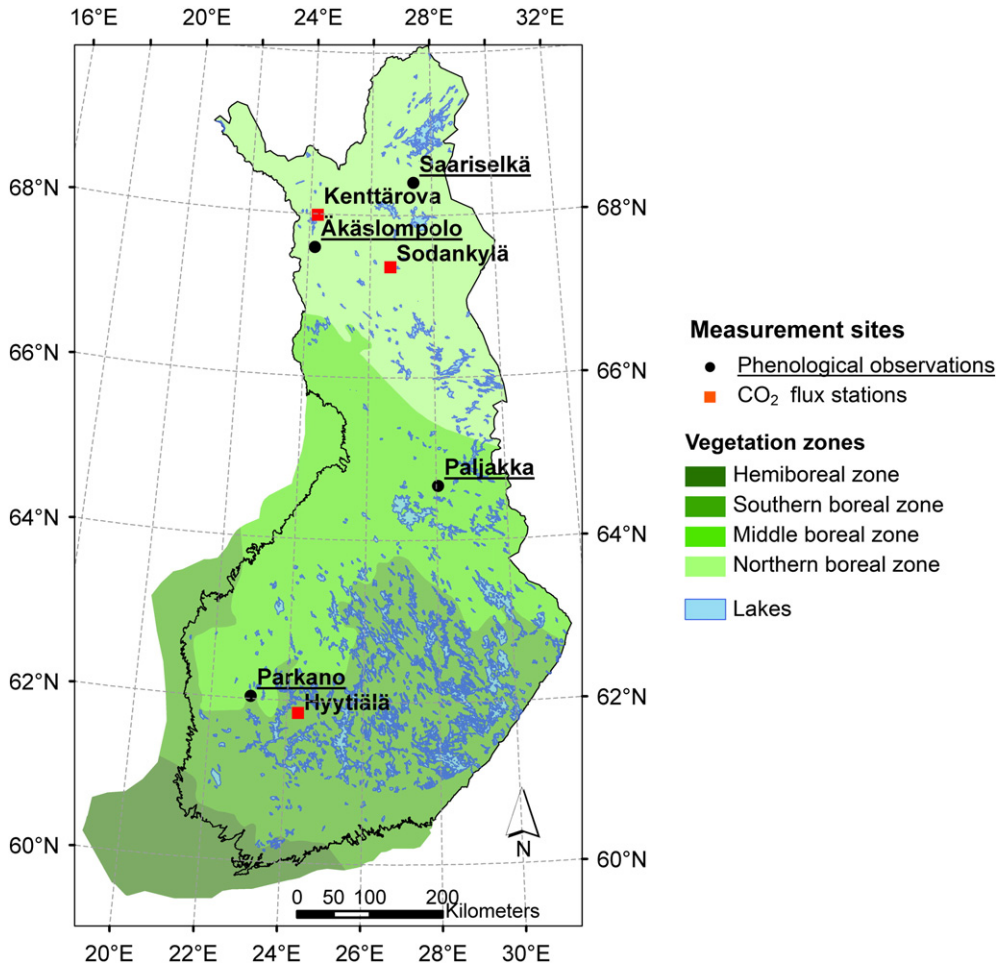

Fig. 1. Location of measurement sites and main phytogeographical zones (Ahti et al., 1968) in Finland.

aiming at the greening-up of the vegetation, phenological observations of beginning of growth of pine trees were also compared at four phenological sites. Satellite-derived GSSDs were evaluated against *in situ* measurements at three sites and the mapping of GSSD was demonstrated in Finland.

2. Data set and methods

2.1. Measurement sites

The measurement sites are located in coniferous forests in Finland, including three CO_2 flux sites and four phenology observation sites (Table 1 and Fig. 1), and stretch from the Southern boreal to the Northern boreal phytogeographical zone. The dominant tree species for all sites is Scots pine (*Pinus sylvestris*), except for Kenttärova with dominance of Norway spruce (*Picea abies*). All sites are located on mineral soils. The snow covered period extends typically from November to May in Northern and from December to April in Southern Finland, covering 6 and 4 months at northern and southern sites, respectively (Kuusisto, 1984).

2.2. CO_2 flux measurements

The *in situ* fluxes of CO_2 were measured by the micrometeorological eddy covariance method, which gives us direct measurements of CO_2 fluxes averaged on an ecosystem scale. In the EC method, the vertical CO_2 flux is obtained as the covariance of the high frequency (10 Hz) observations of vertical wind speed and the CO_2 concentration (Baldocchi, 2003). The eddy covariance measurement systems at Sodankylä and Kenttärova included a USA-1 (METEK GmbH, Elmshorn, Germany) three-axis sonic anemometer/thermometer and a closed-path LI-7000 (Li-Cor., Inc., Lincoln, NE, USA) CO_2/H_2O gas analyzer. In Hyytiälä a Solent 1012R3 anemometer (Gill Instruments Ltd., Lymington, UK) with closed-path LI-6262 analyser (Li-Cor Inc., Lincoln, NE, USA) was used. The measurements were performed 5 to 10 m above the mean forest height. The EC fluxes were calculated as half-hourly averages, taking into account the appropriate corrections. The measurement systems and the post-processing procedures are presented in more detail by Aurela (2005) and Aurela et al. (2009) for Sodankylä and Kenttärova, and by Rannik, Keronen, Hari, and Vesala (2004) and Mammarella et al. (2009) for Hyytiälä. Details on meteorological measurements in Hyytiälä can be found in Vesala et al. (2005). Additional meteorological measurements at each site include precipitation, air temperature at different heights (here we used temperature at 18 m height for Sodankylä and Kenttärova and at 8 m height for Hyytiälä) and soil temperature and volumetric soil liquid water content (SWC) at different depths.

2.3. Determination of GSSD from CO_2 flux measurements

The growing season start date was determined for Sodankylä (2001–2010), Hyytiälä (2001–2010) and Kenttärova (2003–2010) from the continuous CO_2 flux measurement data. GSSD could not be calculated for site Kenttärova for year 2004 due to data gaps. The GSSD is here defined as the day on which the CO_2 uptake exceeds permanently the 15% level of the growing season maximum (Fig. 2). In practice, the GSSD was obtained from the annual cycle of gross photosynthesis index (PI, Aurela, Tuovinen, & Laurila, 2001), which indicates the apparent photosynthetical activity on a daily scale. It is calculated as a

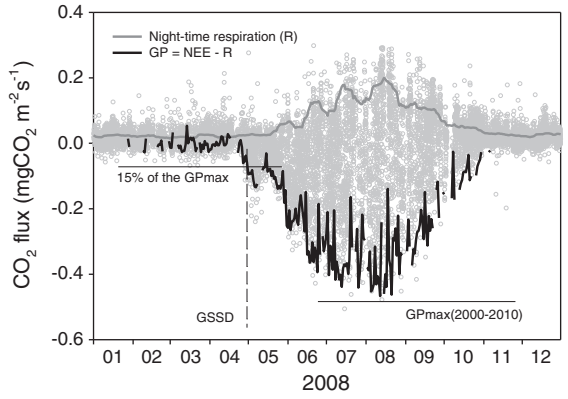

Fig. 2. Determination of GSSD from eddy covariance data (grey circles) at Sodankylä. A common maximum of gross photosynthesis (GPmax) for the whole measurement period (2001–2010) was obtained as the 90th percentile of the daily GP values representing the month of the highest uptake of each year. Daily GP was obtained as a difference of daytime NEE (net ecosystem CO_2 exchange) and night-time respiration. The GSSD for different years was then obtained as the date when daily GP exceeds 15% of this common GPmax.

difference of the daily averages of daytime (Photosynthetic Photon Flux Density (PPFD) > 600 μmol m^{-2} s^{-1}) Net Ecosystem Exchange of CO_2 (NEE) and night-time (PPFD < 20 μmol m^{-2} s^{-1}) respiration and is scaled with the growing season maximum. The obtained index is not actual gross photosynthesis (GP), as the night-time respiration differs from the daytime respiration, but as it is used as a relative measure it provides a reasonable estimate. The growing season maximum is the 90th percentile of the daily GP indexes during the month of highest uptake for the multi-year measurement period. The method used for the determination of GSSD differs from the method used for the same sites by Suni et al. (2003) and Thum et al. (2009). They used instantaneous (30-min) NEE values as compared to daily averages of GP utilized here. However, the progress in photosynthetic activity is typically very fast in these boreal sites, indicating that results are not particularly sensitive to such differences in the method.

2.4. Phenological observations

Phenological observations on pine trees at four sites: Parkano, Paljakka, Äkäslompolo and Saariselkä (Table 1 and Fig. 1), for the years 2001–2010 were obtained from the Finnish Forest Research Institute (METLA). The phenophase (BBCH codes in brackets (Meier, 1997)) beginning of shoot elongation (May shoot, BBCH30) of Scots pine was used in this study. Hereafter, beginning of shoot elongation is referred to as growth of pine start date (GPSD). Phenological observations were carried out twice a week in advanced thinning stands growing on medium fertile soil. The microclimate at the site must be representative of the local climatic conditions. The monitored trees (5 trees) are of local provenance and preferably naturally regenerated. In order to allow accurate observation of shoot elongation, small sized trees in well-illuminated plots were selected. Since 2007 the same trees have been monitored every year, but before that the trees may have changed from year to year. Further details on observations are given in Kubin et al. (2007).

2.5. Snow observations

Daily observations of snow depth and snow coverage for each site were obtained from the nearest weather station, operated by the Finnish Meteorological Institute (FMI). Snow coverage is estimated visually at each station in coarse classes (e-codes) following the definitions by the World Meteorological Organization.

2.6. MODIS data and processing

MODIS-derived FSC and vegetation indices (NDVI and NDWI) were investigated for the use as proxy indicators for GSSD and GPSD. Daily Terra/MODIS Level-1B data (1 km, 500 m and 250 m products) were collected from NASA's Level 1 Land and Atmosphere Archive and Distribution System (LAADS) and/or from the receiving station of FMI in Sodankylä for the period from February to October 2001–2010. Raw instrument data were calibrated to top-of-atmosphere reflectances including sun angle cosine correction. Observations with solar zenith angles greater than 70° and sensor zenith angles greater than 60° were excluded. Calibrated data were projected to geographic latitude/longitude projection (datum WGS-84). Normalized Difference Vegetation Index (NDVI) was computed at 0.0025° resolution with Eq. (1)

$$NDVI = \frac{R_{NIR} - R_{RED}}{R_{NIR} + R_{RED}} \quad (1)$$

where R_{NIR} and R_{RED} refer to near-infrared and red reflectance in MODIS band 2 (841–876 nm) and 1 (620–670 nm), respectively.

In addition to NDVI, the NDWI was computed at 0.005° resolution using Eq. (2)

$$NDWI = \frac{R_{NIR} - R_{MIR}}{R_{NIR} + R_{MIR}} \quad (2)$$

where R_{MIR} refers to middle infrared reflectance in MODIS band 6 (1628–1652 nm).

FSC (0–1) was derived at a pixel size of 0.005 × 0.005° using the SCA*mod* algorithm. The method uses at-satellite observed single-band reflectance and pixel-wise average forest transmissivity for the provision of FSC. With MODIS, band 4 (545–565 nm) reflectance is applied. Clouds were masked in satellite-derived indices using SYKE's operational cloud

Table 2
Characteristics of selected areas from MODIS satellite data.

Site	Number of NDVI pixels[1]	Number of FSC/NDWI pixels[2]	Coniferous forest fraction[3] (%)	Altitude (SD) (m) a.s.l.[4]	Crown cover mean (SD) (%)[5]
Äkäslompolo	55	16	95	329 (23.5)	34 (10.7)
Hyytiälä	175	23	100	170 (3.6)	36 (14.5)
Kenttärova	19	8	95	325 (17.4)	29 (6.4)
Paljakka	65	17	100	292 (29.0)	50 (8.1)
Parkano	11	8	90	144 (6.6)	53(10.3)
Saariselkä	69	21	90	311 (12.1)	32 (2.8)
Sodankylä	27	9	100	213 (11.5)	27 (9.5)

SD, standard deviation.
[1] Resolution of Normalized Difference Vegetation Index (NDVI) pixels is 0.0025°.
[2] Resolution of Fractional Snow Cover (FSC) and Normalized Difference Water Index (NDWI) pixels is 0.005°.
[3] Fraction of coniferous forest was determined based on CORINE Land Cover 2000 for Finland (Härmä et al., 2005).
[4] Altitude is derived from digital elevation model provided by the National Land Survey of Finland with a grid size of 25 × 25 m and a height precision of 2 m.
[5] Crown cover is determined for NDVI pixels and was calculated from field sample plots measured in National Forest Inventory of Finland and Image2006 satellite data (IRS LISS and SPOT XS data) at the resolution of 25 m using the *k*-nearest neighbour (k-NN) classification method (Haakana et al., 2008).

masking algorithm. Observations from two satellite swaths in one day were combined to daily composites using the maximum of the observed vegetation index (Holben, 1986) and the mean value of daily FSC observations.

2.7. Selection of homogenous areas for comparison with in situ observations

For comparison of *in situ* measurements (GSSD and GPSD) with satellite-derived time-series, we selected seven quasi homogenous areas covered with coniferous forest in the vicinity of *in situ* sites (Fig. 1), and that have the same environmental conditions as prevalent at the respective *in situ* site (Table 2). We aimed at large areas in order to minimize the influence of noise and missing observations in satellite data. Thus, the size of the area observed by the satellite sensor varied by site. Selection of areas was based on: (i) fractional cover with coniferous forest (≥90%), determined from CORINE (Coordinated Information on the European Environment) Land Cover 2000 for Finland (CLC 2000, Härmä et al. (2005)) and (ii) altitude. Altitude difference between *in situ* sites and selected MODIS pixels was limited to 50 m and was determined from a digital elevation model for Finland, provided by the National Land Survey of Finland with a pixel size of 25 × 25 m and a height precision of 2 m. In some cases the location of the area was shifted away from the *in situ* site (maximal distance of 10 km), because of inhomogeneity in land cover or close distance to water bodies of the pixel covering the site. MODIS pixels with fractional water coverage were excluded. Crown coverage was in general higher for southern sites than for northern sites, and altitude was higher for northern than for southern sites (Table 2).

2.8. MODIS time-series processing

Vegetation index (NDVI and NDWI) and FSC observations were averaged for all pixels of the seven selected areas (see Table 2). Missing observations in NDVI time-series until mid-February were filled with the NDVI value for full snow cover. Full snow cover NDVI was determined for each pixel based on several observations at the beginning of March 2010. Gaps in daily observations due to cloud cover were filled using linear interpolation and interpolated profiles were smoothed afterwards using the adaptive Savitzky–Golay filter (Chen et al., 2004; Savitzky & Golay, 1964), implemented in TimeSat software, version 2.3 (Jönsson & Eklundh, 2004), with a window size of five days. Linear interpolation was applied to NDWI time-series.

The general shape of snow depletion curves (changes of FSC during the melt season) for an area can be described by an exponential function (Hall & Martinec, 1985) or by fitted splines (Lee, Klein, & Over, 2005). Here, a simple sigmoid function (3) was used to describe the depletion of FSC in spring from full snow cover (FSC = 1) to complete snowmelt (FSC = 0).

$$\mathrm{FSC_f}(t;x_1;x_2) = \frac{1}{1+\exp\left(\frac{t-x_1}{x_2}\right)} \tag{3}$$

where t is the time variable (day), x_1 is the inflection point (day when FSC reaches 0.5) and x_2 controls the rate of change (day) (Fig. 3). The transition from full snow cover to 0% snow cover occurs usually very fast, because an important part of snowmelt occurs before bare ground is exposed (Clark et al., 2006). From visual inspection of satellite-derived time-series of FSC at different locations in Finland, it was found that this simple sigmoid function described well the mean behaviour of snow melt in an area.

Fitting of function (3) to FSC time-series was done in two steps by minimizing the sum of squares of differences between Eq. (3) and measured FSC using the Nelder–Mead Simplex algorithm. Firstly, all observations within the period from February to July were used and initial parameter values were set to $x_1 = 129$ and $x_2 = 1$. Secondly, the time interval for fitting was limited to the melting period and parameters x_1 and x_2 obtained from the first fitting run were used as initial parameters for the second fitting. Using this approach, gaps due to cloud cover can be filled, and noise due to varying viewing and illumination conditions, atmospheric influence, residual clouds or stripes can be smoothed. However, intermittent new snow fall during the ablation period is not captured with this function.

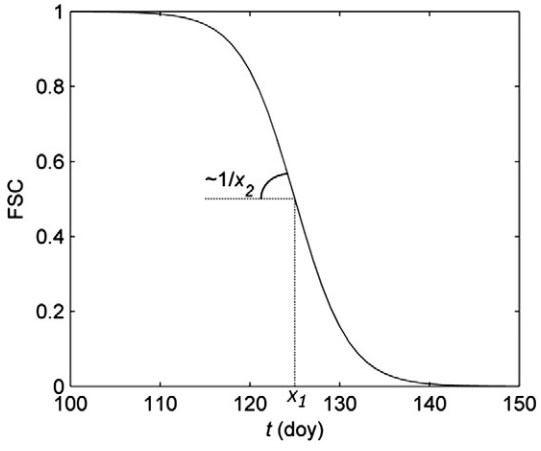

Fig. 3. Example of the sigmoid function (Eq. 3) used to model the FSC time-series during the melting period. It is defined by the inflection point (x_1) and the rate of decrease of FSC at x_1, controlled by x_2.

2.9. Extraction of GSSD and GPSD from MODIS satellite indices

We determined GSSD from time-series of NDVI and $\mathrm{FSC_f}$. GSSD was extracted from NDVI at the time when NDVI's spring-rise began (see Section 3.1). The minimum NDVI during the period from 1st of February to 19th of July was determined from smoothed NDVI profiles and an estimate of the noise level (ε) of the time-series data was defined. Secondly, the condition in Eq. (4a) was applied and the last day fulfilling the condition was determined as GSSD from NDVI:

$$\mathrm{GSSD_{NDVI}} = \arg max_{t\in[32,200]} f(t) := \{t|\mathrm{NDVI}(t) < \mathrm{NDVI_{min}} + \varepsilon\} \tag{4a}$$

with t referring to day of the year (doy), $\mathrm{NDVI_{min}}$ is minimum of NDVI from 1st of February (doy 32) to 19th of July (doy 200) and ε equals 10% of the NDVI amplitude, defined as difference of the maximum NDVI and $\mathrm{NDVI_{min}}$ for each year. For the determination of GSSD from $\mathrm{FSC_f}$ (hereafter denoted as $\mathrm{GSSD_{FSC}}$) a threshold value of 0.99 FSC was applied to Eq. (3), giving the $\mathrm{GSSD_{FSC}}$ as follows:

$$\mathrm{GSSD_{FSC}} = x_1 - \ln(99)x_2. \tag{4b}$$

Due to long periods with cloud cover in spring, $\mathrm{GSSD_{FSC}}$ and $\mathrm{GSSD_{NDVI}}$ could not be obtained for year 2002 in Sodankylä and Kenttärova and for year 2009 in Hyytiälä. Additionally, FSC data was not sufficient for the retrieval of $\mathrm{GSSD_{FSC}}$ for year 2005 in Kenttärova.

For the extraction of GPSD a similar criterion as proposed by Delbart et al. (2005) for determination of the greening-up in the boreal region was used. According to visual comparison of GPSD and NDWI time-series for phenological sites in this study, GPSD occurred earlier than the greening-up (see Section 3.1). GPSD from NDWI was defined as follows:

$$\mathrm{GPSD_{NDWI}} = \arg min_{t\in[32,200]} \mathrm{f(t)} := \{t|\mathrm{NDWI}(t) < \mathrm{NDWI_{min}} + \varepsilon\} \tag{5}$$

with $\mathrm{NDWI_{min}}$ referring to the minimum NDWI and ε equals 20% of NDWI's spring amplitude. The first observation fulfilling the condition

Table 3
Statistical equations used in the evaluation of satellite estimates.

Statistics	Equation
Root mean squared error	$RMSE = \sqrt{\sum_{i=1}^{N} (y_i - \hat{y}_i)^2}/N$
Bias	$B = \sum_{i=1}^{N} (\hat{y}_i - y_i)/N$
Coefficient of determination	$R^2 = \frac{\sum_{i=1}^{N} (\hat{y}_i - \bar{y})^2}{\sum_{i=1}^{N} (y_i - \bar{y})^2}$

y_i is the *in situ* observation and $\hat{y}_i$ is the satellite estimate, $\bar{y}$ is the arithmetic average of y values, and N is the number of observations.

was retained as $GPSD_{NDWI}$. GPSD was determined for the four phenological sites for years with phenological observations (Table 1). Due to long periods with missing data, GPSD was not retrieved for year 2005 in Äkäslompolo and year 2001 in Saariselkä.

Satellite-derived phenological events were evaluated by comparing estimated and *in situ* dates for GSSD and GPSD for all site-years and separately by site. The applied statistical measures were RMSE, the coefficient of determination (R^2) and the bias (B). The equations for statistical measures are presented in Table 3.

3. Results

3.1. Comparison of satellite-derived time-series and in situ observations

Temporal profiles of FSC, NDVI and NDWI in spring 2006 at Sodankylä are shown in Fig. 4. FSC decreased below 1 shortly after the GSSD on 26.04.2006 and when NDVI had a minimum before its spring-rise. NDWI decreased after GSSD. A web-camera image (Fig. 5a) taken from above the canopy at the Nordkalotten Satellite Evaluation co-operation Network (NorSEN) mast (Sukuvaara et al., 2007) in Sodankylä, illustrated that snow had melted around tree trunks at time of GSSD (07.05.2010) and FSC decreased about this time (Fig. 5b). Similar behaviour of GSSD in relation to satellite-indices, as described above, was observed for the southern boreal site Hyytiälä (Fig. 6) and the spruce dominated northern site Kenttärova (not shown); GSSD occurred during snow melt, when depletion of FSC started and NDVI began its spring-rise. GPSD occurred after snowmelt, indicated by an NDWI minimum (Delbart et al., 2005) and a FSC of 0 (Figs. 7 and 8).

Time-series of air and soil temperature, snow depth and SWC in spring together with the time of GSSD are shown in Figs. 9 and 10 for Sodankylä (year 2006) and Hyytiälä (year 2004), respectively. In Sodankylä, air temperature was for several days continuously above 0 °C and soil temperature stayed at 0 °C before GSSD (Fig. 9b). Snow depth was 34 cm and SWC reached 10% (Fig. 9a). In Hyytiälä, air temperatures rose above 0 °C before GSSD and a constant soil temperature of 0 °C was observed during the time period before GSSD (Fig. 10b). Soil temperature increased shortly after that date. SWC was above 20% for the whole period (Fig. 10a).

Meteorological and soil characteristics at time of GSSD were compared between one northern boreal site, Sodankylä, and the southern boreal site Hyytiälä (Table 4). Mean snow depth was higher at Sodankylä (40 cm) than in Hyytiälä (23 cm). Highest snow depth of 65 cm at time of GSSD was found in Sodankylä in year 2005, which was characterized by an intermittent frost period and new snowfall during the snow depletion period. E-code observations at both sites showed similar characteristics related to snow patchiness; the most dominant e-code was 7 (Wet or refrozen snow covering 100% terrain, 11/16 observation years) followed by e-code 6 (Wet or re-frozen snow covering over 50%, but less than 100%, 4/16 observation years). First snow-free spots appear usually early during snow melt at the bases of trees or large rocks (Kuusisto, 1984). These first snow free spots are not depicted by e-code observation at the weather station. Measurements of SWC at sites Hyytiälä and Sodankylä indicated an influx of snow melt water into the soil at time of GSSD (Figs. 9a, 10a and Table 3), increasing the soil temperature and the water availability to trees. Air temperature for both sites was always above 0 °C at time of GSSD, and soil temperature for the upper soil layer ranged between −0.52 and 0.25 °C in Sodankylä (5 cm depth), and 0.07 and 0.77 °C (A-horizon) in Hyytiälä (Table 4). The upper soil layer was usually not completely frozen during the period from February to GSSD in Hyytiälä, but in Sodankylä negative soil temperatures were commonly observed until the influx of snow melt water. The 5-day moving average of air temperature ($T5_{air}$, Table 4), which had previously been used for the prediction of GSSD by Thum et al. (2009), showed differences in $T5_{air}$ at time of GSSD: the average $T5_{air}$ as well as its range was higher for Sodankylä (4.2 °C, 9 °C) than for Hyytiälä (3.6 °C, 5 °C).

3.2. GSSD based on MODIS time-series

Comparisons between satellite-derived GSSD ($GSSD_{NDVI}$ and $GSSD_{FSC}$) and *in situ* dates from three boreal coniferous sites covering observation years 2001 to 2010 are shown in Figs. 11 and 12. Both indices depicted well the growing season start date with a slightly lower RMSE of 5.3 days for $GSSD_{FSC}$ compared to 6.3 days for $GSSD_{NDVI}$. The range of GSSD from the southern to northern sites was captured with the indicators $GSSD_{NDVI}$ and $GSSD_{FSC}$, but data points were grouped for the northern and southern sites, especially for $GSSD_{NDVI}$, implying that inter-annual differences at a specific site are less well captured by $GSSD_{NDVI}$. The satellite-indicators detected on average the growing season start 1–2 days later than *in situ* observations (Table 5). High R^2 (>0.8) values resulted also from the large range between northern and southern sites in time of GSSD and we examined therefore also site-wise correspondence (Table 5). Correlations between $GSSD_{NDVI}$ and *in situ* dates were significant only for site Hyytiälä, whereas significant site-wise correlations between $GSSD_{FSC}$ and *in situ* dates were obtained for sites Sodankylä and Hyytiälä (R^2>0.7), as well as a higher R^2 for site Kenttärova. Note that for the Kenttärova site only 6 years were available for comparison. The combination of observations for the two northern boreal sites led to an R^2 of 0.53 for $GSSD_{FSC}$. The lower R^2 for northern sites is mainly due to larger errors for the Kenttärova site with dominance of spruce. Latest GSSD according to flux measurements was observed in Kenttärova on 23rd of May 2008. Both satellite-indices suggested a start of season too early in that year with 14 days and 9 days differences for $GSSD_{FSC}$ and $GSSD_{NDVI}$, respectively. This was also the largest error obtained for $GSSD_{FSC}$. Actual recovery lagged snow melt in that year (zero cm snow depth on 19th of May 2008), which might be due to a cold spell, as observed by air temperature observations in Kenttärova. Largest error for $GSSD_{NDVI}$ of 16 days in year 2003 was as well found for this site.

3.3. GPSD based on MODIS time-series

Results for the determination of $GPSD_{NDWI}$ for four phenological sites according to Eq. (5) are shown in Table 6 and Fig. 13. Satellite-derived $GPSD_{NDWI}$ for 29 site-years accounted only for 54% of the variation *in situ* observations and data point were dispersed and grouped by site (Fig. 13). Site-wise correlations were not significant and R^2 remained below 0.5 for three out of four sites (Table 6), hence inter-annual variability at site-level cannot be captured. Mean GPSD for each phenological site could nevertheless be depicted by NDWI time-series with B ranging from −2 to 3 days for different sites (Table 6). We observed differences in B between sites from southern and central Finland (Parkano, Paljakka), and northern sites (Äkäslompolo, Saariselkä), with an early B (2–3 days) for the first two stations and a late B (2–3 days) for the latter.

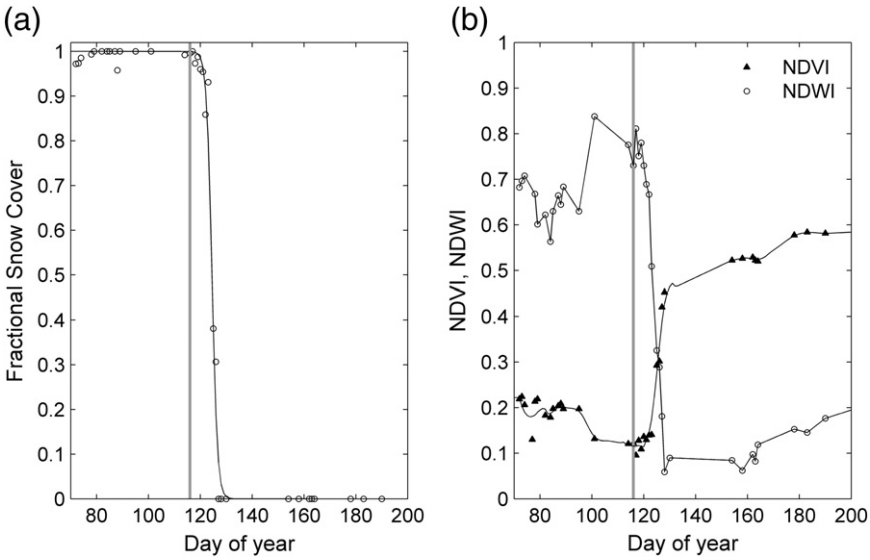

Fig. 4. Satellite-derived time-series of vegetation indices and snow cover at Sodankylä during the period from mid-March to July 2006: (a) Fractional Snow Cover, FSC_f; (b) NDVI and NDWI. The vertical grey line indicates GSSD on 26.04.2006.

3.4. Demonstration of the mapping of GSSD for Finland

The results described in previous sections suggest that the MODIS-derived estimate of FSC can be used as proxy for the spatial mapping of GSSD (Fig. 12). This is shown in Fig. 14 by applying Eq. (4b) to time-series of FSC_f. In order to reduce noise and gaps due to cloud cover in FSC time-series, daily observations from pixels with at least 70% coniferous forest coverage were aggregated to a grid size of 0.1 × 0.1°. The aggregation of time-series to a coarser grid was found useful for the mapping of the autumn colouring from MODIS time-series (Rauste et al., 2007). Furthermore, maps are intended for comparison with the spatial distribution of modelled GSSD by a land surface scheme forced with regional meteorological data, which are typically calculated at a coarser grid size than MODIS satellite observations. Daily FSC observations were averaged for each grid cell after removing outliers based on the criterion of two standard deviations. Function (3) was fitted to average FSC time-series of each grid cell and $GSSD_{FSC}$ was extracted from the fitted profile based on Eq. (4b). The delay of spring photosynthetic recovery in coniferous forest in Finland from Southwest to Northeast is illustrated in Fig. 14. This is in correspondence with the climatic gradient. The map for year 2007 showed an earlier GSSD for most areas in Finland compared to year 2004. Thermal spring in 2007 began about one month earlier than average in Finland; mean temperatures in March 2007 were higher than normal (Finnish Meteorological Institute, 2012).

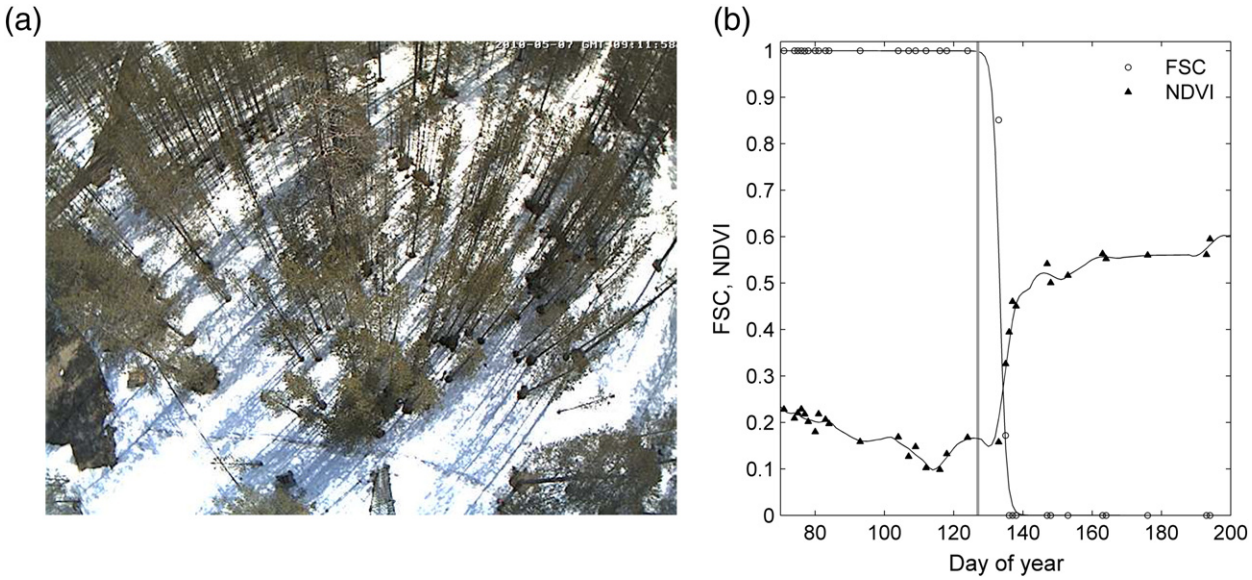

Fig. 5. (a) Web-camera photograph taken from the NorSEN mast (30 m height) in Sodankylä on GSSD (07.05.2010). (b) FSC and NDVI time-series in Sodankylä in spring 2010. The vertical grey line indicates GSSD.

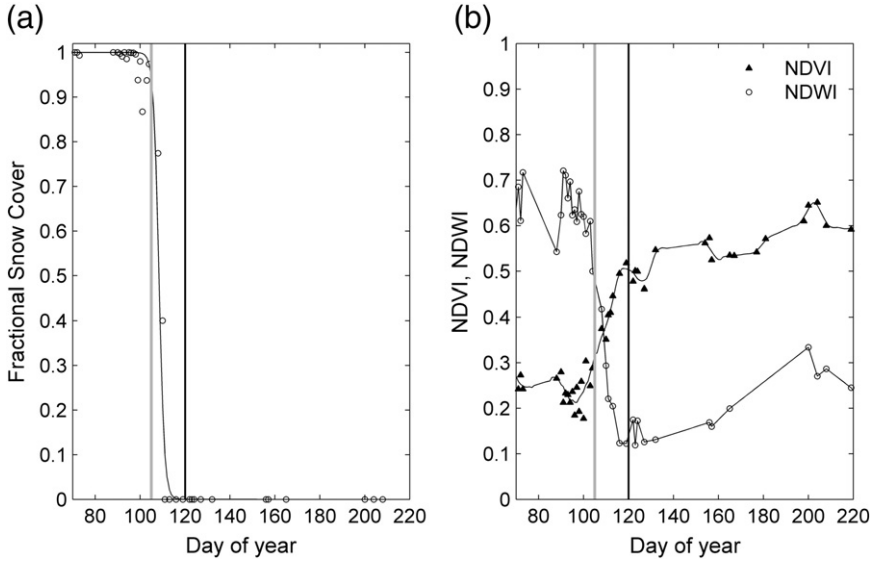

Fig. 6. Satellite-derived time-series of vegetation indices and snow evolution at Hyytiälä from mid-March–August in 2004: (a) Fractional Snow Cover, FSC_f and (b) NDVI and NDWI. The grey vertical line indicates GSSD (14.04.2004) and the black vertical line GPSD (Parkano, 29.04.2004).

4. Discussion

4.1. Snow melt as indicator for photosynthetic recovery

We found correspondence of the time of photosynthetic recovery in boreal evergreen conifers with the time during snowmelt when ground starts to be exposed as observed by satellite-derived indices. Our findings are supported by the results by Thum et al. (2009), who reported that the beginning of growing season in boreal conifers corresponded well with the decrease of MODIS/Terra + Aqua albedo observations. Furthermore, Kimball, McDonald, Running, and Frolking (2004) found good correspondence between timing of seasonal snow melt observed by radar backscatter measurements and growing season initiation (start of xylem sap flow), as well as with ecosystem process model simulations for boreal, maritime and subalpine sites in Northern America.

Photosynthetic recovery in boreal conifers is mainly controlled by increasing air temperature (Mäkelä et al., 2004; Suni et al., 2003), which also controls the snow melt. The response to air temperature seems to be slower in colder northern sites than southern boreal sites (Gea-Izquierdo et al., 2010; Suni et al., 2003; Thum et al., 2009), which may be attributed to deeper frozen soils in northern sites than in southern sites and a longer time lag between the rise in air and soil temperatures. Also in this study, $T5_{air}$ at time of GSSD was higher for the northern site Sodankylä than at the Hyytiälä site; northern sites Kenttärova and Sodankylä are characterized by a larger snow pack and lower soil temperatures in winter (Figs. 9 and 10) than the Hyytiälä site. Besides favourable air temperature, the isothermality of the snow pack is a pre-requisite for full springtime recovery of photosynthetic uptake, permitting continuous daytime percolation of melted snow water through the vertical snow profile and availability of snow melt water to trees (Kimball et al., 2004; Monson et al., 2005). The GSSD, determined here at a fixed rate of growing season GPP, occurred when a high amount of snow had already melted and melt water percolated into the soil as indicated by relatively high levels of soil water content (Table 4 and Figs. 9a, 10a).

4.2. Detection of GSSD from MODIS time-series

The depletion of snow cover in spring was used as indicator for the extraction of GSSD from daily time-series of FSC and NDVI for

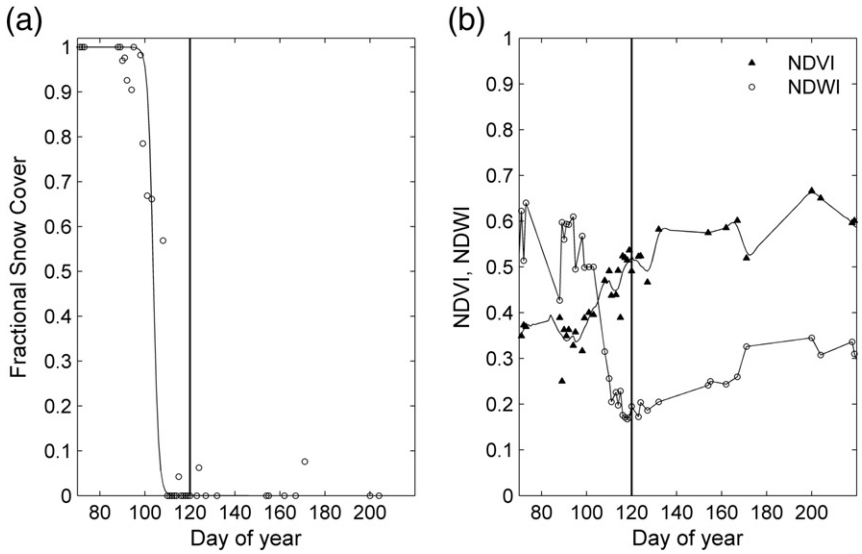

Fig. 7. Satellite-derived time-series of vegetation indices and snow evolution at Parkano from mid-March–August in 2004: (a) Fractional Snow Cover, FSC_f and (b) NDVI and NDWI. The black vertical line indicates GPSD (29.04.2004).

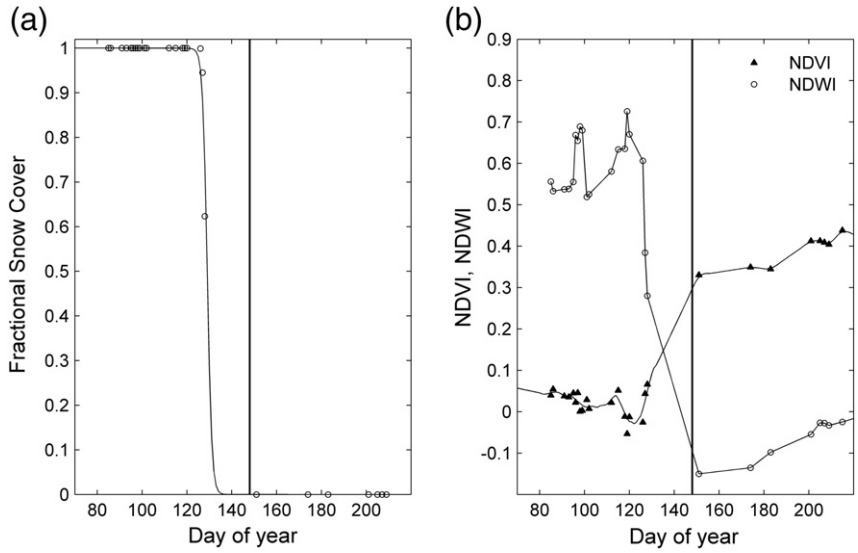

Fig. 8. Satellite-derived time-series of vegetation indices and snow evolution at Saariselkä from mid-March–August in 2004: (a) Fractional Snow Cover, FSC_f and (b) NDVI and NDWI. The black vertical line indicates GPSD (27.05.2004).

three boreal evergreen coniferous sites in Finland (Figs. 4a and 6a). $GSSD_{FSC}$ was better suited for the detection of GSSD than $GSSD_{NDVI}$ (Table 5, Figs. 11, 12). FSC time-series used in this study were derived with the SCA*mod* method, which provides low omission errors for full snow cover as well as for low snow fractions (Metsämäki et al., 2012), which is an advantage for the detection of timing of melting onset and snow clearance. Furthermore, the method compensates for the effect of different crown coverage of the forest sites (Table 2) by using forest transmissivity in the retrieval of FSC (Metsämäki et al., 2005). In contrast, the NDVI winter level is dependent on crown coverage, e.g. showing higher NDVI values for southern boreal sites (Figs. 6b, 7b) than for the northern sites (Figs. 4b and 8b). This was accounted for by using a relative NDVI threshold for the detection of GSSD, which is similar to approaches for the greening-up of temperate deciduous forests (Badeck et al., 2004; White et al., 1997).

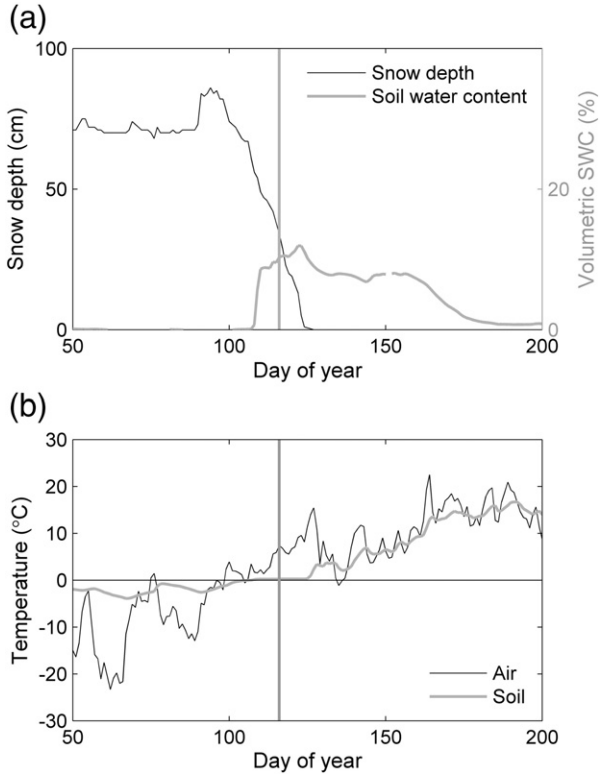

Fig. 9. Time-series of meteorological and soil parameters at Sodankylä for the period from mid-February to July 2006: (a) Snow depth (cm) and volumetric SWC (%) and (b) daily air and soil temperature (°C). The vertical grey line indicates GSSD on 26.04.2006. Soil water content and soil temperature were measured at 5 cm depth.

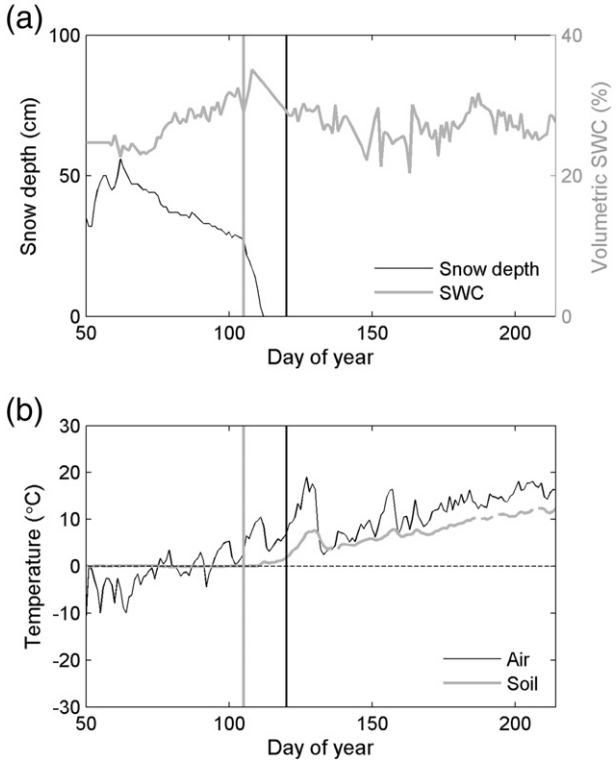

Fig. 10. Time-series of mean daily meteorological and soil parameters at Hyytiälä for the period from mid-February to August 2004: (a) Snow depth (cm) and volumetric SWC (%) and (b) air and soil temperature (°C). The vertical grey line indicates GSSD on 14.04.2004 and the black vertical line GPSD (Parkano, 29.04.2004). Soil water content and soil temperature were measured for soil A-horizon (0–10 cm depth).

Table 4
Growing season start dates (GSSD) together with meteorological and soil characteristics on GSSD at CO_2 flux measurement stations in Sodankylä and Hyytiälä.

Site	Year	GSSD (doy)	Snow depth (cm)	e-code	SWC (%)	$T5_{air}$ (°C)	T_{soil} (°C)
Hyytiälä	2001	95	25	7	32	4.33	0.17
	2002	102	20	6	36	6.22	0.77
	2003	107	15	5	29	5.14	0.35
	2004	105	27	6	29	3.51	0.07
	2005	93	19	*	30	5.13	0.10
	2006	104	33	7	24	2.69	0.17
	2007	75	14	7	29	1.46	0.16
	2008	90	34	7	32	4.12	0.64
	2009	97	*	7	30	1.11	0.15
	2010	90	*	7	19	2.75	0.25
Sodankylä	2001	118	34	7	*	4.39	−0.29
	2002	114	43	7	*	6.63	−0.52
	2003	127	20	6	*	2.63	−0.27
	2004	120	37	6	*	5.07	0.01
	2005	126	65	7	*	0.04	0.04
	2006	116	34	7	10	6.32	0.23
	2007	113	44	7	25	0.24	0.06
	2008	122	43	*	*	9.43	0.22
	2009	120	*	*	11	5.01	0.24
	2010	127	*	*	22	1.76	0.25

SWC, volumetric soil water content. $T5_{air}$, 5 day moving average of daily air temperature. T_{soil}, daily soil temperature measured at 5 cm depth in Sodankylä and for the A-horizon (0–10 cm depth) in Hyytiälä.
Snow depth and e-codes for Hyytiälä and Sodankylä were obtained from meteorological stations Juupajoki Hyytiälä and Sodankylä Arctic Research Centre of FMI, respectively. An asterisk (*) denotes missing observations. Description for e-code values: 5, Snow covering over 0%, but less than 50% of the terrain; 6, Wet or re-frozen snow covering over 50%, but less than 100% of the terrain; 7, Wet or re-frozen snow covering 100% of the terrain.

We used large homogenous areas near *in situ* sites for the retrieval of satellite-indicators. Better correlations were obtained for comparisons between satellite-derived and ground observation of phenology for homogenous vegetation covers, and it was suggested that land cover heterogeneity is a main error source (Doktor, Bondeau, Koslowski, & Badeck, 2009; Maignan et al., 2008). In addition, due to the mismatch between the spatial scales of satellite and field observations (Liang, Schwartz, & Fei, 2011) and the averaging out of errors in coarser measurements, higher spatial representation (coarser resolution) of satellite estimates led to better correlations with seasonal transitions derived from EC measurements (Garrity et al., 2011). Satellite-estimates from single pixels are more likely to be influenced by noise and missing values. Reducing the size of the area for the retrieval of $GSSD_{FSC}$ for the Hyytiälä site from 23 to 9 pixels ($0.005 \times 0.005°$ resolution) decreased accuracy slightly, with lower R^2 (0.71) and higher B (2.9 days). Missing data is especially relevant for northern latitudes with long periods of cloud cover and a fast development of vegetation in spring (Beck et al., 2006). A daily coverage of satellite observations is beneficial in capturing the timing of snow cover decrease, as snowmelt proceeds very fast after the peak of melting; the period corresponding to partial snow cover in forest lasts in northern, central and southern Finland about 15 days in average (Kuusisto, 1984). However, even with daily observations and large areas, data gaps in cloud-free MODIS observations for the spring period in some years were too long for the retrieval of satellite-proxy indicators (e.g. time period in Sodankylä with missing observations was more than a month in 2002).

Most available methods for the retrieval of the beginning of the growing season in the boreal zone from optical satellite observations aimed at the detection of the greening-up of deciduous vegetation with reference to the bud burst of deciduous trees (Delbart, Le

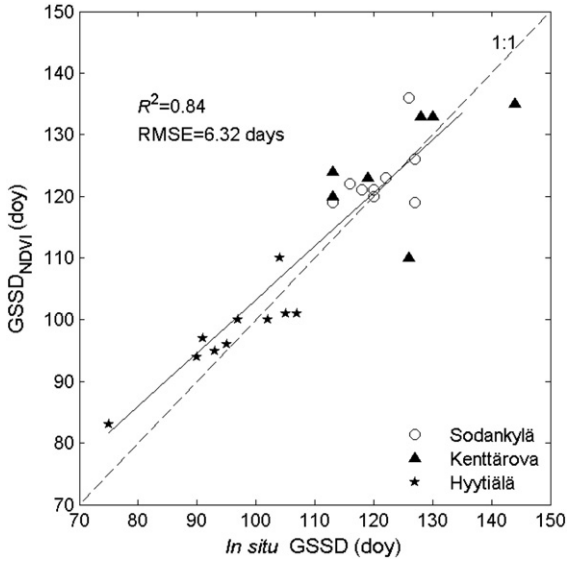

Fig. 11. Comparison of *in situ* measurements of GSSD with estimates derived from time-series of NDVI ($GSSD_{NDVI}$). Doy is day of year. Black line shows linear regression line between *in situ* data and $GSSD_{NDVI}$.

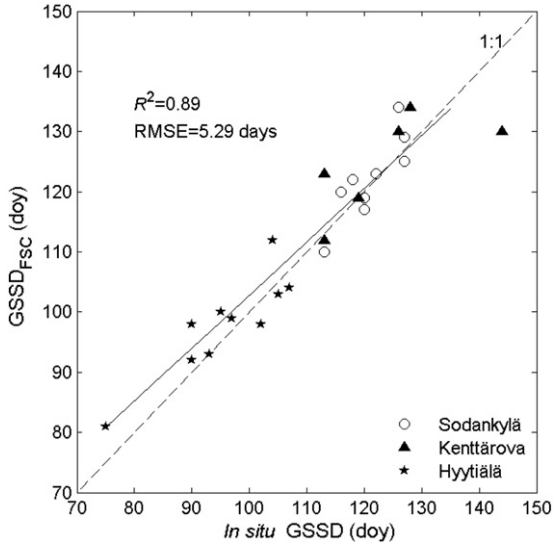

Fig. 12. Comparison of *in situ* measurements of GSSD with estimates derived from time-series of Fractional Snow Cover ($GSSD_{FSC}$). Doy is day of year. Black line shows linear regression line between *in situ* data and $GSSD_{FSC}$.

Table 5
Growing season start date (GSSD) as measured by NDVI and FSC and as defined from CO_2 flux measurement sites.

Site	*In situ*	Estimate from NDVI				Estimate from FSC			
	Mean GSSD (doy)	# y	Mean $GSSD_{NDVI}$ (doy)	R^2	*B* (day)	# y	Mean $GSSD_{FSC}$ (doy)	R^2	*B* (day)
Hyytiälä	96	10	98	0.80**	2	10	98	0.79**	2
Kenttärova	124	7	125	0.30	1	6	125	0.50	1
Sodankylä	121	9	123	0.25	2	9	122	0.73**	1
All sites	112	26	114	0.84**	2	25	113	0.89**	1

#y, number of years when both *in situ* data and satellite observations were available for comparison. GSSD, growing season start date from CO_2 flux measurements. Doy, day of year. $GSSD_{NDVI}$, growing season start date from NDVI. $GSSD_{FSC}$, growing season start date from Fractional Snow Cover. R^2, coefficient of determination, * significant at 5% level, ** significant at 1% level. *B* is bias.

Toan, Kergoat, & Fedotova, 2006; Delbart et al., 2005, 2008; Karlsen, Elvebakk, Høgda, & Johansen, 2006; Karlsen et al., 2007, 2008; Shutova et al., 2006). Therefore, these results are not directly comparable to our results. Recently, Gonsamo et al. (2012) developed a new phenological index (PI) combining the advantages of NDVI and Normalized Difference Infrared Index (NDII), similar to NDWI. The results based on PI for boreal coniferous sites in Canada, with a similar range of start of season dates as in this study, showed low correlation and an RMSE of 17.2 days. Estimates of growing season initiation from radar observations occurred up to 10 days earlier than site measurements of growing season initiations (onset of xylem sap flow) for two years of observations across 10 evergreen forest study sites in Northern America (Kimball et al., 2004). The observed RMSE from radar estimates was with 9.9 days (Kimball et al., 2004) and 8.7 days (Bartsch, Kidd, Wagner, & Bartalis, 2007) higher than for $GSSD_{FSC}$ as well as $GSSD_{NDVI}$ (Figs. 11 and 12).

Since air temperature is commonly used as predictor for GSSD, we compared our results also with air-temperature derived estimates of GSSD. Good accuracy was achieved for northern latitudes when optimizing temperature threshold values for a specific site. Suni et al. (2003) found good agreement between the commencement day of photosynthesis (*P*, defined here from NEE) and the day when the threshold values of $T5_{air}$ (3.3 °C and 6.5 °C for Hyytiälä and Sodankylä, respectively) was exceeded. Temperature-derived *P* deviated from observations in the range of 0–2 and 2–3 days for Hyytiälä and Sodankylä, respectively. However, applying a common threshold to five different sites in the boreal region led to a prediction error of 8.6 days, compared to 5.3 days for $GSSD_{FSC}$ in this study (Fig. 12), and systematically later observed *P* for the northern sites and *vice versa* for the warmer Hyytiälä site. The bias of $GSSD_{FSC}$ was low for all three sites in Finland, showing only a one day larger *B* for Hyytiälä than for the northern sites (Table 5). In a study including more site-years, but applying the same method as Suni et al. (2003) for the determination of *P*, prediction error for $T5_{air}$ ranged between 1–5 and 2–22 days for Hyytiälä and Sodankylä, respectively (Thum et al., 2009). Prediction of *P* from $T5_{air}$ in Hyytiälä preceded observed *P* always. RMSE for site-specific thresholds of $T5_{air}$ for 11 sites-years from Hyytiälä, Sodankylä and Kenttärova was 7.3 days.

4.3. Detection of GPSD from MODIS time-series

We derived GPSD from daily NDWI time-series for four sites with dominance of pine trees (Fig. 13). The method applied here does not actually detect the beginning of shoot growth, but GPSD is related to the end of snow melt as described by the decrease of NDWI. Mean $GPSD_{NDWI}$ occurred before the greening-up of deciduous species determined by the method of Delbart et al. (2005). Early bias in $GPSD_{NDWI}$ for northern sites (Äkäslompolo and Saariselkä) (Table 6) suggested an overlap of snowmelt and beginning of shoot growth as also reported by Gonsamo et al. (2012). Changes in NDVI as well as NDWI time-series after the end of snow melt were very small (Figs. 7 and 8), which corresponds to observations by Jönsson et al. (2010). Vegetation indices specifically developed for the tracking of seasonal change in leaf area index of evergreen coniferous forest (e.g. Stenberg, Rautiainen, Manninen, Voipio, & Smolander, 2004) might be better suited for the determination of GPSD and should be considered in further studies.

4.4. Mapping of GSSD in Finland

Satellite-derived maps for the start of the growing season (defined as greening-up) in Fennoscandia were presented by Beck et al. (2006)

Table 6
Growth of pine start date (GPSD) as measured by NDWI and as observed at phenological sites.

Site	# y	Mean GPSD (doy)	Mean $GPSD_{NDWI}$ (doy)	R^2	*B* (day)
Äkäslompolo	5	145	149	0.18	3
Paljakka	10	139	136	0.05	−3
Parkano	9	121	119	0.05	−2
Saariselkä	5	143	145	0.74	2
All sites	29	136	134	0.54**	−2

#y, number of years when both *in situ* and satellite data were available for comparison. GPSD, growth of pine start date from phenological observation. Doy, day of year. $GPSD_{NDWI}$, growth of pine start date from Normalized Difference Water Index. R^2, coefficient of determination, ** significant at 1% level. *B* is bias.

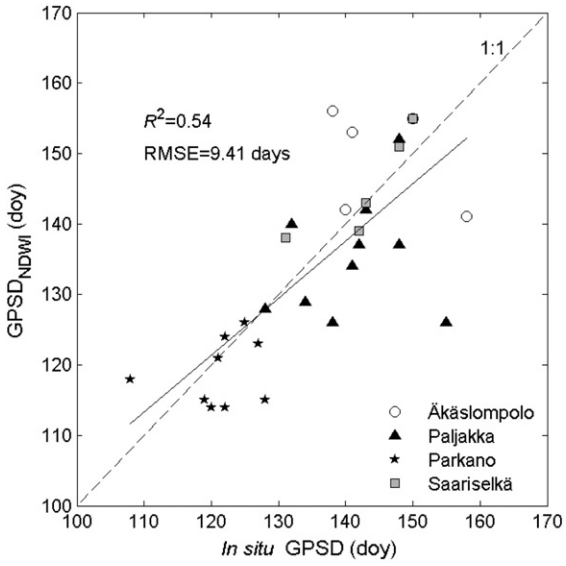

Fig. 13. Comparison of *in situ* measurements of GPSD with estimates derived from time-series of NDWI ($GPSD_{NDWI}$). Doy is day of year. Black line shows linear regression line between *in situ* data and $GPSD_{NDWI}$.

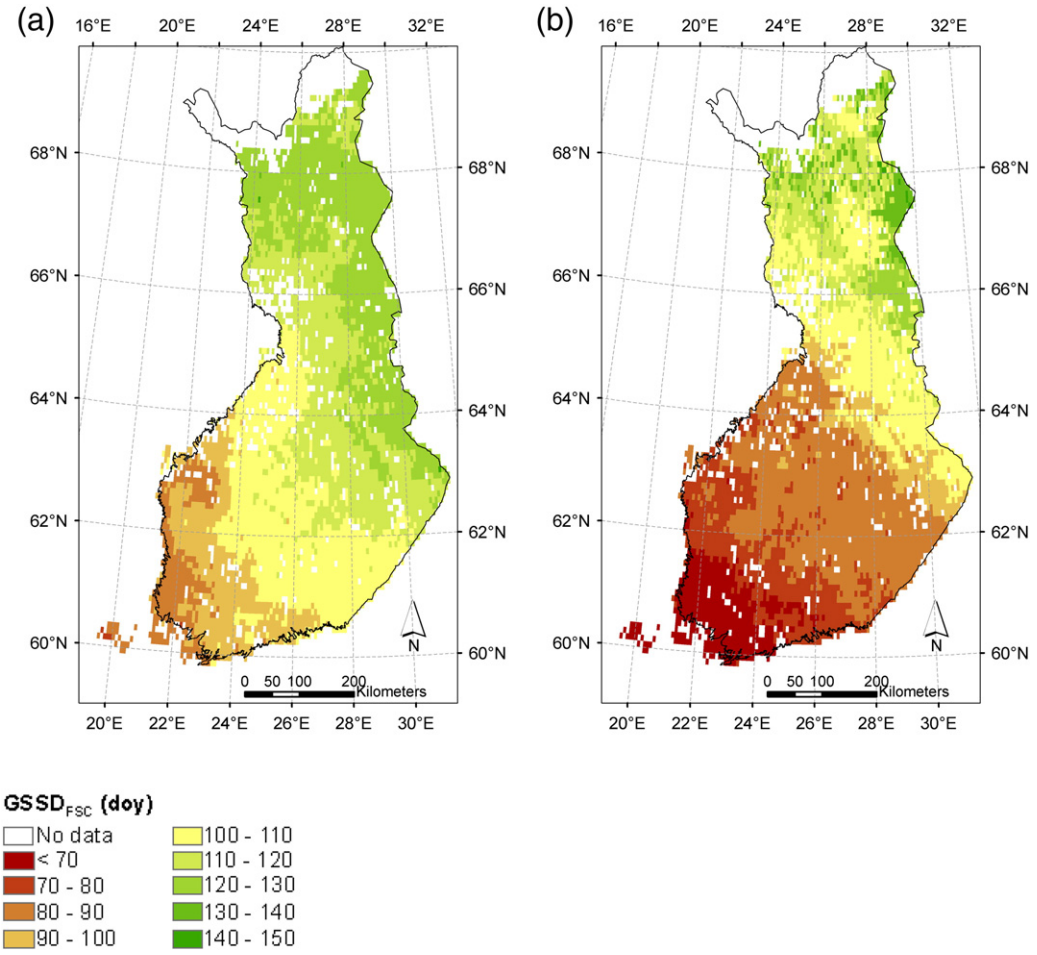

Fig. 14. Maps of satellite-derived growing season start date from Fractional Snow Cover ($GSSD_{FSC}$) for years (a) 2004 and (b) 2007 in evergreen coniferous forest in Finland.

and Karlsen et al. (2007). Here, we targeted at the detection of recovery of photosynthetic activity in evergreen coniferous forest, thus results are not comparable in their timing. The greening-up in Southern Finland occurred on average (years 1982–2002) between 1 and 15 May in the results of Karlsen et al. (2007). In this study, $GSSD_{FSC}$ was observed as early as mid-March to mid-April (Fig. 14). However, the spatial patterns were in general consistent between greening-up and GSSD as well as with modelled bud-burst of birch (Bennie, Kubin, Wiltshire, Huntley, & Baxter, 2010) and followed the climatic gradient. GSSD maps suggested a very early start of the growing season in the south-western coastal areas (Fig. 14; hemiboreal zone, Fig. 1) in Finland. The applicability of the method for mapping of GSSD based on FSC to the hemiboreal zone and also to the southern part of the boreal zone may fail in winters with very low snow depth, when the direct effect of low temperature or the combination of low temperature and high light (Delpierre et al., 2012; Gea-Izquierdo et al., 2010) are more important for the restriction of photosynthetic recovery in spring. In contrast to other studies, we separated the coniferous forest from other land cover classes for the mapping of GSSD and considered only MODIS pixels with dominant coniferous fraction. Although, maps were presented at coarse resolution ($0.1 \times 0.1°$), this approach has the advantage that different methods can be applied for areas with different vegetation cover, thus allowing comparisons with GSSD calculated by a land surface scheme for different plant functional types.

5. Conclusion

In this study, MODIS-derived time-series of NDVI, NDWI and FSC were compared with *in situ* measurements of the start of growing season determined from CO_2 flux measurements and with phenological observations of the beginning of pine growth at four sites in Finland in order to find suitable satellite indicators for these events. The time during snow melt when ground starts to be exposed corresponded well with GSSD ($R^2 > 0.8$, RMSE <7 days) at three flux measurement sites in boreal evergreen coniferous forest. The satellite-indicator can be derived from both NDVI and FSC time-series, but with higher accuracy from FSC time-series. This is important for the mapping of the beginning of the growing season in the boreal region, as current optical satellite-based methods (e.g. Delbart et al., 2008; Karlsen et al., 2008) rely mainly on validation with observations of bud burst of deciduous trees, which lag behind the beginning of photosynthetic recovery in coniferous trees. The satellite-derived indicator $GSSD_{FSC}$ did not show systematic differences between northern and the southern sites and estimation errors seem to be lower compared to air temperature derived indicators when using common thresholds for sites in different zones of the boreal region. Furthermore, the mapping of $GSSD_{FSC}$ was demonstrated in this paper. In contrast, the satellite-derived indicator $GPSD_{NDWI}$ showed only low correlation with phenological observations of pine growth and cannot be applied for the mapping of this event. The calibration of satellite indicators to GSSD from CO_2 flux measurements opens the possibility to evaluate the spatial distribution of land-surface model-derived beginning of growing season against satellite observations.

Acknowledgements

The work was funded by EU Life + project SnowCarbo (LIFE + 07/ENV/FIN/000133), which is gratefully acknowledged. MODIS Level-1B

data were acquired from LAADS web, located at Goddard Space Flight Center of the National Aeronautics and Space Administration (NASA) http://ladsweb.nascom.nasa.gov/. We thank Eero Kubin (Finnish Forest Research Institute, Finland) for phenological observations and Wolfgang Mehl (Joint Research Centre, Italy) for IDL software routines. Furthermore, we thank Tea Thum (Finnish Meteorological Institute, Finland) for useful comments to the manuscript and data related to the growing season start based on air temperature.

References

Ahti, T., Hämet-Ahti, L., & Jalas, J. (1968). Vegetation zones and their sections on northwestern Europe. *Annales Botanica Fennica*, *5*, 169–211.

Aurela, M. (2005). *Carbon dioxide exchange in subarctic ecosystems measured by a micrometeorological technique.* (PhD thesis). Helsinki, Finland: Finnish Meteorological Institute.

Aurela, M., Lohila, A., Tuovinen, J. -P., Hatakka, J., Riutta, T., & Laurila, T. (2009). Carbon-dioxide exchange on a northern boreal fen. *Boreal Environmental Research*, *14*, 699–710.

Aurela, M., Tuovinen, J. -P., & Laurila, T. (2001). Net CO_2 exchange of a subarctic mountain birch ecosystem. *Theoretical and Applied Climatology*, *70*, 135–148.

Badeck, F. -W., Bondeau, A., Böttcher, K., Doktor, D., Lucht, W., Schaber, J., & Sitch, S. (2004). Responses of spring phenology to climate change. *New Phytologist*, *162*, 295–309.

Baldocchi, D.D. (2003). Assessing the eddy covariance technique for evaluating carbon dioxide exchange rates of ecosystems: Past, present and future. *Global Change Biology*, *9*, 479–492.

Bartsch, A., Kidd, R. A., Wagner, W., & Bartalis, Z. (2007). Temporal and spatial variability of the beginning and end of daily spring freeze/thaw cycles derived from scatterometer data. *Remote Sensing of Environment*, *106*, 360–374.

Beck, P.S. A., Atzberger, C., Høgda, K. A., Johansen, B., & Skidmore, A. K. (2006). Improved monitoring of vegetation dynamics at very high latitudes: A new method using MODIS NDVI. *Remote Sensing of Environment*, *100*, 321–334.

Beck, P.S. A., Jönsson, P., Høgda, K. -A., Karlsen, S. R., Eklundh, L., & Skidmore, A. K. (2007). A ground-validated NDVI dataset for monitoring vegetation dynamics and mapping phenology in Fennoscandia and the Kola peninsula. *International Journal of Remote Sensing*, *28*, 4311–4330.

Bennie, J., Kubin, E., Wiltshire, A., Huntley, B., & Baxter, R. (2010). Predicting spatial and temporal patterns of bud-burst and spring frost risk in north-west Europe: The implications of local adaptation to climate. *Global Change Biology*, *16*, 1503–1514.

Bergh, J., & Linder, S. (1999). Effects of soil warming during spring on photosynthetic recovery in boreal Norway spruce stands. *Global Change Biology*, *5*, 245–253.

Chen, J., Jönsson, P., Tamura, M., Gu, Z., Matsushita, B., & Eklundh, L. (2004). A simple method for reconstructing a high-quality NDVI time-series data set based on the Savitzky–Golay filter. *Remote Sensing of Environment*, *91*, 332–344.

Clark, M. P., Slater, A. G., Barrett, A. P., Hay, L. E., McCabe, G. J., Rajagopalan, B., & Leavesley, G. H. (2006). Assimilation of snow covered area information into hydrologic and land-surface models. *Advances in Water Resources*, *29*, 1209–1221.

Delbart, N., Kergoat, L., Le Toan, T., L'Hermitte, J., & Picard, G. (2005). Determination of phenological dates in boreal regions using normalized difference water index. *Remote Sensing of Environment*, *97*, 26–38.

Delbart, N., Le Toan, T., Kergoat, L., & Fedotova, V. (2006). Remote sensing of spring phenology in boreal regions: A free of snow-effect method using NOAA-AVHRR and SPOT-VGT data (1982–2004). *Remote Sensing of Environment*, *101*, 52–62.

Delbart, N., Picard, G., Le Toan, T., Kergoat, L., Quegan, S., Woodward, I. A. N., Dye, D., & Fedotova, V. (2008). Spring phenology in boreal Eurasia over a nearly century time scale. *Global Change Biology*, *14*, 603–614.

Delpierre, N., Soudani, K., François, C., Le Maire, G., Bernhofer, C., Kutsch, W., Misson, L., Rambal, S., Vesala, T., & Dufrêne, E. (2012). Quantifying the influence of climate and biological drivers on the interannual variability of carbon exchanges in European forests through process-based modelling. *Agricultural and Forest Meteorology*, *154–155*, 99–112.

Doktor, D., Bondeau, A., Koslowski, D., & Badeck, F. -W. (2009). Influence of heterogeneous landscapes on computed green-up dates based on daily AVHRR NDVI observations. *Remote Sensing of Environment*, *113*, 2618–2632.

Drebs, A., Nordlund, A., Karlsson, P., Helminen, J., & Rissanen, P. (2002). *Climatological statistics of Finland 1971–2000*. Helsinki: Finnish Meteorological Institute.

Duchemin, B., Goubier, J., & Courrier, G. (1999). Monitoring phenological key stages and cycle duration of temperate deciduous forest ecosystems with NOAA/AVHRR data. *Remote Sensing of Environment*, *67*, 68–82.

Finnish Meteorological Institute (2012). Weather in recent years. http://en.ilmatieteenlaitos.fi/weather-in-recent-years (Accessed on 07/05/2012)

Ganguly, S., Friedl, M.A., Tan, B., Zhang, X., & Verma, M. (2010). Land surface phenology from MODIS: Characterization of the Collection 5 global land cover dynamics product. *Remote Sensing of Environment*, *114*, 1805–1816.

Gao, B. -C. (1996). NDWI—A normalized difference water index for remote sensing of vegetation liquid water from space. *Remote Sensing of Environment*, *58*, 257–266.

Garrity, S. R., Bohrer, G., Maurer, K. D., Mueller, K. L., Vogel, C. S., & Curtis, P.S. (2011). A comparison of multiple phenology data sources for estimating seasonal transitions in deciduous forest carbon exchange. *Agricultural and Forest Meteorology*, *151*, 1741–1752.

Gea-Izquierdo, G., Mäkelä, A., Margolis, H., Bergeron, Y., Black, T. A., Dunn, A., Hadley, J., Paw U, K. T., Falk, M., Wharton, S., Monson, R., Hollinger, D. Y., Laurila, T., Aurela, M., McCaughey, H., Bourque, C., Vesala, T., & Berninger, F. (2010). Modeling acclimation of photosynthesis to temperature in evergreen conifer forests. *New Phytologist*, *188*, 175–186.

Gonsamo, A., Chen, J. M., Price, D. T., Kurz, W. A., & Wu, C. (2012). Land surface phenology from optical satellite measurement and CO_2 eddy covariance technique. *Journal of Geophysical Research*, *117*, G03032.

Gutman, G. G. (1991). Vegetation indices from AHVRR: An update and future prospects. *Remote Sensing of Environment*, *35*, 121–136.

Haakana, M., Hatunen, S., Härmä, P., Kallio, M., Katila, M., Kiiski, T., Mäkisara, K., Peräsaari, J., Piepponen, H., Repo, R., Teiniranta, R., Tomppo, E., & Törmä, M. (2008). Finnish CORINE 2006-project: determining changes in land cover in Finland between 2000 and 2006. *SPIE Europe Remote Sensing Congress. Cardiff, Wales, United Kingdom*.

Hall, D. K., & Martinec, J. (1985). *Remote sensing of ice and snow*. London: Chapman and Hall.

Hall, D. K., & Riggs, G. A. (2007). Accuracy assessment of the MODIS snow products. *Hydrological Processes*, *21*, 1534–1547.

Härmä, P., Teiniranta, R., Törmä, M., Repo, R., Järvenpää, E., & Kallio, E. (2005). *CLC2000 Finland: final report*. Finnish Environment Institute, Geoinformatics and Land Use Division.

Holben, B. (1986). Characteristics of maximum-value composite images from temporal AVHRR data. *International Journal of Remote Sensing*, *7*, 1417–1434.

Huemmrich, K. F., Black, T. A., Jarvis, P. G., McCaughey, J. H., & Hall, F. G. (1999). High temporal resolution NDVI phenology from micrometeorological radiation sensors. *Journal of Geophysical Research: Atmospheres*, *104*, 27935–27944.

Jönsson, P., & Eklundh, L. (2004). TIMESAT-a program for analyzing time-series of satellite sensor data. *Computers & Geosciences*, *30*, 833–845.

Jönsson, A.M., Eklundh, L., Hellström, M., Bärring, L., & Jönsson, P. (2010). Annual changes in MODIS vegetation indices of Swedish coniferous forests in relation to snow dynamics and tree phenology. *Remote Sensing of Environment*, *114*, 2719–2730.

Karlsen, S. R., Elvebakk, A., Høgda, K. A., & Johansen, B. (2006). Satellite-based mapping of the growing season and bioclimatic zones in Fennoscandia. *Global Ecology and Biogeography*, *15*, 416–430.

Karlsen, S., Solheim, I., Beck, P., Høgda, K., Wielgolaski, F., & Tømmervik, H. (2007). Variability of the start of the growing season in Fennoscandia, 1982–2002. *International Journal of Biometeorology*, *51*, 513–524.

Karlsen, S. R., Tolvanen, A., Kubin, E., Poikolainen, J., Høgda, K. A., Johansen, B., Danks, F. S., Aspholm, P., Wielgolaski, F. E., & Makarova, O. (2008). MODIS-NDVI-based mapping of the length of the growing season in northern Fennoscandia. *International Journal of Applied Earth Observation and Geoinformation*, *10*, 253–266.

Kaufmann, R. K., Zhou, L., Knyazikhin, Y., Shabanov, N. V., Myneni, R. B., & Tucker, C. J. (2000). Effect of orbital drift and sensor changes on the time series of AVHRR Vegetation Index Data. *IEEE Transactions on Geoscience and Remote Sensing*, *38*, 2584–2597.

Kimball, J. S., McDonald, K. C., Running, S. W., & Frolking, S. E. (2004). Satellite radar remote sensing of seasonal growing seasons for boreal and subalpine evergreen forests. *Remote Sensing of Environment*, *90*, 243–258.

Kubin, E., Kotilainen, E., Poikolainen, J., Hokkanen, T., Nevalainen, S., Pouttu, A., Karhu, J., & Pasanen, J. (2007). *Fenologisen havaintoverkon seurantaohjeet*. Finnish Forest Research Institute.

Kuusisto, E. (1984). *Snow accumulation and snowmelt in Finland*. Helsinki, Finland: National Board of Waters.

Lee, S., Klein, A. G., & Over, T. M. (2005). A comparison of MODIS and NOHRSC snow-cover products for simulating streamflow using the Snowmelt Runoff Model. *Hydrological Processes*, *19*, 2951–2972.

Liang, L., Schwartz, M.D., & Fei, S. (2011). Validating satellite phenology through intensive ground observation and landscape scaling in a mixed seasonal forest. *Remote Sensing of Environment*, *115*, 143–157.

Maignan, F., Bréon, F. M., Bacour, C., Demarty, J., & Poirson, A. (2008). Interannual vegetation phenology estimates from global AVHRR measurements: Comparison with in situ data and applications. *Remote Sensing of Environment*, *112*, 496–505.

Mäkelä, A., Hari, P., Berninger, F., Hänninen, H., & Nikinmaa, E. (2004). Acclimation of photosynthetic capacity in Scots pine to the annual cycle of temperature. *Tree Physiology*, *24*, 369–376.

Mammarella, I., Launiainen, S., Grönholm, T., Keronen, P., Pumpanen, J., Rannik, Ü., & Vesala, T. (2009). Relative humidity effect on the high frequency attenuation of water vapour flux measured by a closed path eddy covariance system. *Journal of Atmospheric and Oceanic Technology*, *26*, 1856–1866.

Meier, U. (Ed.). (1997). *BBCH-Monograph. Growth stages of mono- and dicotyledonous plants*. Berlin: Blackwell.

Melaas, E. K., Richardson, A.D., Friedl, M.A., Dragoni, D., Gough, C. M., Herbst, M., Montagnani, L., & Moors, E. (2013). Using FLUXNET data to improve models of springtime vegetation activity onset in forest ecosystems. *Agricultural and Forest Meteorology*, *171–172*, 46–56.

Metsämäki, S. J., Anttila, S. T., Huttunen, M. J., & Vepsäläinen, J. M. (2005). A feasible method for fractional snow cover mapping in boreal zone based on a reflectance model. *Remote Sensing of Environment*, *95*, 77–95.

Metsämäki, S., Mattila, O. -P., Pulliainen, J., Niemi, K., Luojus, K., & Böttcher, K. (2012). An optical reflectance model-based method for fractional snow cover mapping applicable to continental scale. *Remote Sensing of Environment*, *123*, 508–521.

Monson, R., Sparks, J., Rosenstiel, T., Scott-Denton, L., Huxman, T., Harley, P., Turnipseed, A., Burns, S., Backlund, B., & Hu, J. (2005). Climatic influences on net ecosystem CO_2 exchange during the transition from wintertime carbon source to springtime carbon sink in a high-elevation, subalpine forest. *Oecologia*, *146*, 130–147.

Moulin, S., Kergoat, L., Viovy, N., & Dedieu, G. (1997). Global-scale assessment of vegetation phenology using NOAA/AVHRR satellite measurements. *Journal of Climate*, *10*, 1154–1155.

Rannik, Ü., Keronen, P., Hari, P., & Vesala, T. (2004). Estimation of forest atmosphere CO_2 exchange by eddy covariance and profile techniques. *Agricultural and Forest Meteorology*, *126*, 141–155.

Rauste, Y., Astola, H., Häme, T., Berglund, R., Sirro, L., Veijonen, T., Veikkanen, B., Kubin, E., & Aulamo, O. (2007). Automatic monitoring of autumn colours using MODIS data. *IEEE International Geoscience and Remote Sensing Symposium, IGARSS 2007. Barcelona, Spain* (pp. 1295–1298).

Reed, B. C., Brown, J. F., Vanderzee, D., Loveland, T. R., Merchant, J. W., & Ohlen, D. O. (1994). Measuring phenological variabilty from satellite imagery. *Journal of Vegetation Sciences*, *5*, 703–714.

Richardson, A.D., Andy Black, T., Ciais, P., Delbart, N., Friedl, M.A., Gobron, N., Hollinger, D. Y., Kutsch, W. L., Longdoz, B., Luyssaert, S., Migliavacca, M., Montagnani, L., William Munger, J., Moors, E., Piao, S., Rebmann, C., Reichstein, M., Saigusa, N., Tomelleri, E., Vargas, R., & Varlagin, A. (2010). Influence of spring and autumn phenological transitions on forest ecosystem productivity. *Philosophical Transactions of the Royal Society B: Biological Sciences*, *365*, 3227–3246.

Richardson, A.D., Hollinger, D. Y., Dail, D. B., Lee, J. T., Munger, J. W., & O'keefe, J. (2009). Influence of spring phenology on seasonal and annual carbon balance in two contrasting New England forests. *Tree Physiology*, *29*, 321–331.

Riggs, G. A., Hall, D. K., & Salomonson, V. V. (2006). *MODIS snow products user guide to collection 5.* Boulder, CO, USA: National Snow & Ice Data Centre.

Savitzky, A., & Golay, M. J. E. (1964). Smoothing and differentiation of data by simplified least squares procedures. *Analytical Chemistry*, *36*, 1627–1639.

Sellers, P. J. (1985). Canopy reflectance, photosynthesis and transpiration. *International Journal of Remote Sensing*, *6*, 1335–1372.

Sevanto, S., Suni, T., Pumpanen, J., Grönholm, T., Kolari, P., Nikinmaa, E., Hari, P., & Vesala, T. (2006). Wintertime photosynthesis and water uptake in a boreal forest. *Tree Physiology*, *26*, 749–757.

Shutova, E., Wielgolaski, F., Karlsen, S., Makarova, O., Berlina, N., Filimonova, T., Haraldsson, E., Aspholm, P., Fløa, L., & Høgda, K. (2006). Growing seasons of Nordic mountain birch in northernmost Europe as indicated by long-term field studies and analyses of satellite images. *International Journal of Biometeorology*, *51*, 155–166.

Soudani, K., le Maire, G., Dufrêne, E., François, C., Delpierre, N., Ulrich, E., & Cecchini, S. (2008). Evaluation of the onset of green-up in temperate deciduous broadleaf forests derived from Moderate Resolution Imaging Spectroradiometer (MODIS) data. *Remote Sensing of Environment*, *112*, 2643–2655.

Stenberg, P., Rautiainen, M., Manninen, T., Voipio, P., & Smolander, S. (2004). Reduced simple ratio better than NDVI for estimating LAI in Finnish pine and spruce stands. *Silva Fennica*, *38*, 3–14.

Sukuvaara, T., Pulliainen, J., Kyrö, E., Suokanerva, H., Heikkinen, P., & Suomalainen, J. (2007). Reflectance spectroradiometer measurement system in 30 meter mast for validating satellite images. *IEEE 2007 International Geoscience and Remote Sensing Symposium (IGARSS), Sensing and understanding our planet. Barcelona, Spain* (pp. 1524–1528).

Suni, T., Berninger, F., Vesala, T., Markkanen, T., Hari, P., Mäkelä, A., Ilvesniemi, H., Hänninen, H., Nikinmaa, E., Huttula, T., Laurila, T., Aurela, M., Grelle, A., Lindroth, A., Arneth, A., Shibistova, O., & Lloyd, J. (2003). Air temperature triggers the recovery of evergreen boreal forest photosynthesis in spring. *Global Change Biology*, *9*, 1410–1426.

Thum, T., Aalto, T., Laurila, T., Aurela, M., Hatakka, J., Lindroth, A., & Vesala, T. (2009). Spring initiation and autumn cessation of boreal coniferous forest CO_2 exchange assessed by meteorological and biological variables. *Tellus B*, *61*, 701–717.

Vesala, T., Suni, T., Rannik, Ü., Keronen, P., Markkanen, T., Sevanto, S., Grönholm, T., Smolander, S., Kulmala, M., Ilvesniemi, H., Ojansuu, R., Uotila, A., Levula, J., Mäkelä, A., Pumpanen, J., Kolari, P., Kulmala, L., Altimir, N., Berninger, F., Nikinmaa, E., & Hari, P. (2005). Effect of thinning on surface fluxes in a boreal forest. *Global Biogeochemical Cycles*, *19*, GB2001.

Wang, Q., Tenhunen, J., Dinh, N. Q., Reichstein, M., Vesala, T., & Keronen, P. (2004). Similarities in ground- and satellite-based NDVI time series and their relationship to physiological activity of a Scots pine forest in Finland. *Remote Sensing of Environment*, *93*, 225–237.

White, M.A., De Beurs, K. M., Didan, K., Inouye, D. W., Richardson, A.D., Jensen, O. P., O'Keefe, J., Zhang, G., Nemani, R. R., Van Leeuwen, W. J.D., Brown, J. F., De Wit, A., Schaepman, M., Lin, X., Dettinger, M., Bailey, A. S., Kimball, J., Schwartz, M.D., Baldocchi, D.D., Lee, J. T., & Lauenroth, W. K. (2009). Intercomparison, interpretation, and assessment of spring phenology in North America estimated from remote sensing for 1982–2006. *Global Change Biology*, *15*, 2335–2359.

White, M.A., Thornton, P. E., & Running, S. W. (1997). A Continental Phenology Model for Monitoring Vegetation Responses to Interannual Climatic Variability. *Global Biogeochemical Cycles*, *11*, 217–234.

Wu, S. H., Jansson, P. -E., & Kolari, P. (2012). The role of air and soil temperature in the seasonality of photosynthesis and transpiration in a boreal Scots pine ecosystem. *Agricultural and Forest Meteorology*, *156*, 85–103.